Korean J. Chem. Eng., 33(5), 1720-1727 (2016)
DOI: 10.1007/s11814-015-0295-4

pISSN: 0256-1115
eISSN: 1975-7220

Effect of sorbitan monostearate concentration on the thermal, mechanical and drug release properties of oleogels

Sai Sateesh Sagiri*, Uvanesh Kasiviswanathan*, Gauri Shankar Shaw*, Meenakshi Singh*, Arfat Anis,†, and Kunal Pal*,†**

*Department of Biotechnology and Medical Engineering, National Institute of Technology, Rourkela-769008, Orissa, India
**SABIC Polymer Research Center, Department of Chemical Engineering, King Saud University, Riyadh-11421, Saudi Arabia
(*Received 11 September 2015 • accepted 23 December 2015*)

Abstract−The current study describes the effect of the concentration of Span 60 (gelator) on the properties of oleogels. Mustard oil was chosen as the representative vegetable oil. Microscopy showed that an increase in the gelator concentration resulted in the increase in the gelator network density. Thermal studies (crystallization kinetics and differential scanning calorimetry) indicated a 2-stage crystallization process. An increase in the gelator proportion resulted in the increase in the compatibility amongst the oleogel components. The formation of gelator network was governed by the interaction amongst the hydroxyl groups of Span 60. A variation in the gelator proportion resulted in the alteration in the d-spacing, crystallite size and lattice strain. The variation in the above-mentioned properties was found to affect the viscoelastic properties of the oleogels as was predicted from the Weichert model. The drug release studies suggested that the drug diffusion due to the gelator network relaxation during drug release was predominant as compared to the Fickian diffusion. The results suggested that it is possible to alter not only the release profile of drugs but also the physical properties (of the oleogels) by tailoring the gelator concentration.

Keywords: Oleogels, Mustard Oil, Biocompatibility, Span 60, Controlled Drug Delivery

INTRODUCTION

Gel-based delivery systems have gained importance for their ability to control the release of the drugs and increased stability of the formulations. Gels have been defined as semi-solid formulations that consist of a solid component and a liquid component. A 3-dimensional network is formed by the solid component, regarded as gelator. The architecture of the network is dependent on the concentration and the nature of the gelators. The commonly used gelators include stearic acid, sorbitan monooleate (Span 60), sorbitan monostearate, 12-hydroxy stearic acid, β-sitosterol and γ-oryzanol. The liquid component is accommodated within this 3-dimensional network. The liquid component may either be polar (in case of hydrogels) or apolar (in case of organogels) in nature. The various apolar solvents used for the development of organogels include kerosene oil, sunflower oil, mustard oil and mineral oil [1-3]. If the apolar liquid is vegetable oil, then the formulations are regarded as oleogels.

In this study, Span 60 was used as the gelator. Span 60 is an FDA approved non-ionic surfactant having hydrophilic lipophilic balance (HLB) of 4.7. It promotes the formation of water-in-oil emulsions. Due to its non-ionic nature, Span 60 is biocompatible and non-irritant [4-6]. In addition to its afore-mentioned properties, Span 60 has been tried as a structuring agent for developing formulations for cosmetic, food and pharmaceutical applications [7-11]. Formulations that contain Span 60 as the structuring agent are thermodynamically stable for long durations [3,12]. Span 60 based oleogels can modulate the release property of the bioactive agents (e.g., oligopeptides, polypeptides, cyclosporin, and salicylic acid) [13].

Refined mustard oil was used as the representative oil in this study. Mustard oil, which is obtained from the seeds of *Brassica nigra*, has been traditionally used in household cooking. Apart from its utility in cooking, it has also been used in various clinical conditions due to its antimicrobial, rubefacient and anti-cancer activities [14-16]. But nowadays its use in clinical conditions is decreasing because of the difficulty in handling the oil, typically, spillage. This may be overcome by structuring the oil using a suitable organogelator [17]. Hence, in the present study, attempts were made to use Span 60 as the organogelator to modify the texture of the refined mustard oil. Refined mustard oil is a GRAS (Generally Regarded as Safe) compound, approved by the US FDA for external (topical) and food applications [18]. Mustard paste has been extensively applied topically to relieve the pain [18,19]. The use of the oil as an adjuvant for immune-enhancing delivery system is well documented [16].

The present study discusses the development of Span 60 based oleogels. The effect of Span 60 concentration on the properties of the oleogels were studied in-depth. The oleogels were characterized using microscopic, FTIR, XRD, thermal and mechanical studies. Ciprofloxacin, a wide-spectrum antibiotic, was incorporated within the oleogels. The release properties of the drug from the oleogels were also studied in-depth.

†To whom correspondence should be addressed.
E-mail: kpal.nitrkl@gmail.com, aarfat@ksu.edu.sa

MATERIALS AND METHODS

1. Materials

Span 60 was procured from Loba Chemie, Mumbai, India. Ciprofloxacin was a gift from Aristo Pharmaceutical (P) Ltd., India. Refined mustard oil (Dhara Kachi Ghani Mustard Oil) was procured from Mother Dairy Fruit & Vegetable Pvt. Ltd., Uttar Pradesh, India. Double distilled water was used throughout the studies.

2. Preparation of Organogels

The oleogels were prepared by varying the proportions of mustard oil and Span 60. The proportion of the Span 60 was varied from 1% to 22% (w/w) in the formulations. The samples were prepared by dissolving accurately weighed Span 60 in mustard oil (70 °C), kept on stirring on a magnetic stirrer (100 rpm) until a homogeneous solution was obtained. The resulting solution was allowed to cool to 25 °C in a temperature-controlled thermal cabinet. The samples were stored at room temperature (25 °C) for further analysis. Drug loaded oleogels were prepared in a similar fashion. Ciprofloxacin was used as a model antimicrobial drug. 1% (w/v) ciprofloxacin was dispersed in mustard oil and was used for the preparation of the drug-loaded oleogels.

3. Microscopic Studies

The microstructures of the thin smears of the oleogels were analyzed under bright- field microscope (DM 750, LEICA, Germany).

4. Thermal Studies

The crystallization kinetics of the oleogels was studied using an optical density measuring device. 10 g of the oleogels was transferred to 15 ml culture bottles. The oleogels were heated to 60 °C and subsequently allowed to cool to room temperature.

The thermal properties of the oleogels were studied using differential scanning calorimeter (DSC F3 Maia, Netzsch, Germany). The analysis was done in the temperature range of 10 °C and 100 °C. The thermal scanning was done at a rate of 1 °C/min under an inert atmosphere of nitrogen gas. 10-15 mg of the oleogels was used for the analysis.

5. FTIR Studies

Chemical interactions amongst the components of the oleogels were studied using an FTIR, spectrophotometer (Alpha-E, Bruker, USA), operated in attenuated total reflectance (ATR) mode. The scanning was done in the IR wavelength range of 450-4,000 cm^{-1}.

6. XRD Studies

The oleogels were scanned in the range of 5-50° 2θ using X-ray diffractometer (Ultima IV Multipurpose X-Ray Diffraction System, Rigaku, USA). The scan rate was set to 2° 2θ/min.

7. Mechanical Studies

Gel strength (3 mm probe), spreadability (spreadability rig) and stress relaxation (spreadability rig) properties of the oloegels were determined using a static mechanical tester (Stable Microsystems, TA-HD plus, U.K). In all the experiments, the speed of the probe was kept at 1 mm/sec.

8. *In vitro* Drug Release Studies

The drug release studies were carried out in a modified Franz's diffusion cell. The donor and the receptor were separated by dialysis membrane (MW: 60 kDa, Himedia, Mumbai). The donor was filled with 1.5 g of the drug-loaded oleogels. The receptor contained 50 ml of water (37 °C). The receptor fluid was kept on stirring at 100 rpm. The receptor fluid was replaced at regular intervals. The study was conducted for 5 h. The collected samples were analyzed using UV-vis spectrometer (Shimadzu UV 1601 r) at a wavelength of 271 nm for determining ciprofloxacin concentration.

RESULTS AND DISCUSSION

1. Preparation of Oleogels

Span 60 was dissolved in mustard oil (70 °C) and subsequently cooled to room temperature (25 °C). The percentage of Span 60 was varied in the range of 1% (w/w) and 22% (w/w) to determine the minimum amount of Span 60 required to immobilize mustard oil (*critical gelling concentration*; CGC) [20]. At concentrations below 17% (w/w), Span 60 was not able to induce gelation. Hence, 17% (w/w) of Span 60 was regarded as the CGC for mustard oil. During the cooling process of the hot Span 60 solution, the solution became cloudy due to the initiation of the crystallization of Span 60 in the oil phase. The cloudy suspension remained as fluid at room temperature if the concentration of Span 60 was <17% (w/w). If the concentration of Span 60 was ≥17%, the cloudy suspensions were transformed into semi-solid formulations at room temperature and were regarded as oleogels. The oleogels did not flow under gravity when the culture bottles were inverted [21] (Fig. S1). The oleogels were yellow and may have been related to the color of the mustard oil. The oleogels had a slight odor and were smooth and "oily" to the touch. The composition of the oleogels, which were used for further analysis, have been tabulated in Table 1.

2. Microscopic Studies

The micrographs of the oleogels showed the presence of the network structure formed of solid fibers (Fig. 1). The density of the solid fibers was higher as the concentration of Span 60 was increased. This type of network structure is formed by self-assembly of the gelator molecules (here Span 60) during the cooling process. When the hot solution of the gelator is cooled, there is a formation of nucleation points. These nucleation points serve as the starting point for the growth of the gelator crystals. The growing crystals get interconnected to form a network structure. Similar observation was also made in our study (Fig. S1). The interconnected networks, so formed, are responsible for arresting the movement of the apolar liquid (here mustard oil) [22]. An increase in the gelator concentration resulted in the increase in the fiber diameter and length.

2-1. Thermal Properties

The absorption profile of the hot Span 60 solution is shown in Fig. 2(a). A preliminary analysis of the absorption profiles suggested

Table 1. Composition of organogels selected for further analysis

Sample	Span 60 (% w/w)	Mustard oil (% w/w)	CFX (% w/w)
F1	17.0	83.0	--
F2	20.0	80.0	--
F3	22.0	78.0	--
F1C	17.0	82.0	1.0
F2C	20.0	79.0	1.0
F3C	22.0	77.0	1.0

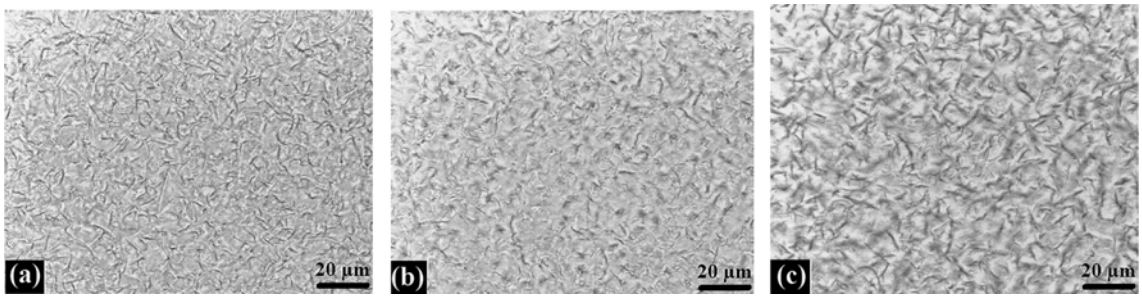

Fig. 1. Bright field micrographs of: (a) F1, (b) F2, and F3.

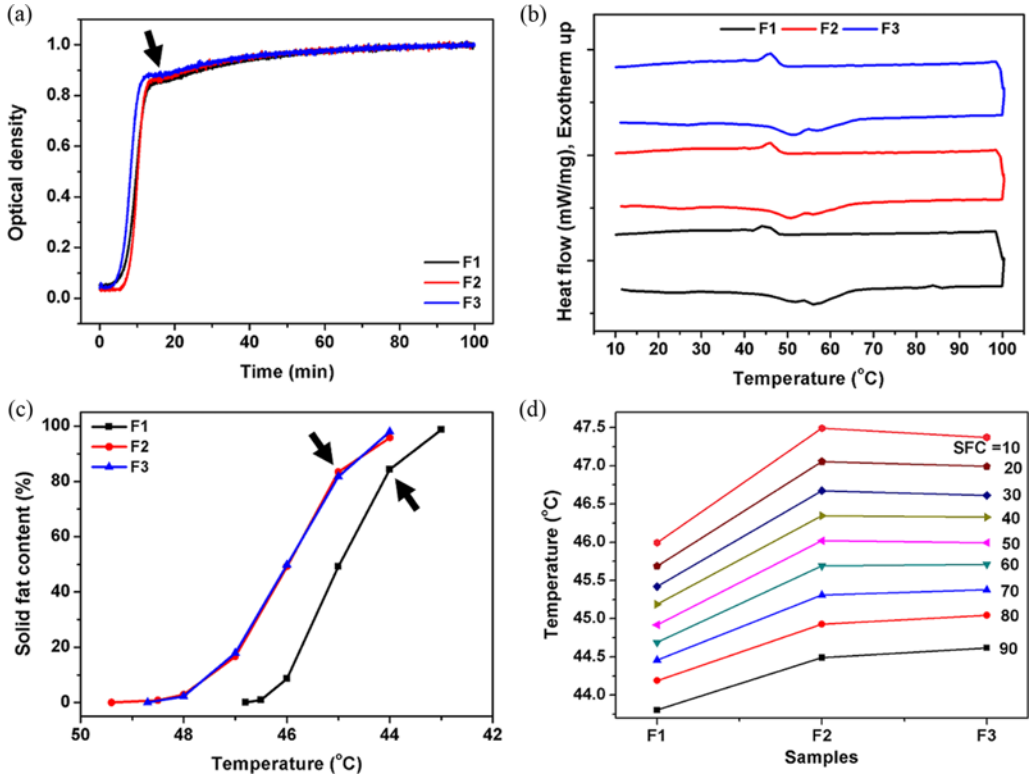

Fig. 2. Thermal analysis of the oleogels. (a) Absorption profiles during solidification process, (b) thermograms of the formulations, (c) solid fat content profile, and (d) isosolid diagram.

two-stage crystallization process of Span 60. The initial crystallization profile was a sigmoidal. After reaching a near saturation (marked by arrow), a second inflection was seen. This suggested a probability of the presence of secondary crystallization process. To ascertain this, the samples were subjected to DSC analysis. The thermograms of the formulations showed the presence of two melting and crystallization events (Fig. 2(b); Table S1). The results confirmed the prediction of secondary crystallization process during the cooling process, as was observed from the absorption profiles. An increase in the Span 60 concentration resulted in the increase in the enthalpies (considering both the peaks together) during the melting and the crystallization processes. This suggested that the thermal stability of the oleogels was increased with the increase in the Span 60 concentration. The changes in the solid fat content (SFC) during the crystallization process were calculated from the crystallization thermograms [23]. The profiles of the changes in the SFC are shown in Fig. 2(c). An analysis of the SFC profiles suggested that the crystallization of F1 started at lower temperature as compared to F2 and F3, respectively. Even the crystallization process in F2 and F3 was complete at higher temperatures. The profiles indicated a sudden change in the SFC profile near completion (marked by arrows), which also supported the secondary crystallization process. The isosolid diagram suggested that the profiles were relatively parallel to each other when the Span 60 concentration was higher (Fig. 2(d)) [24]. The results indicated that an increase in the Span 60 concentration resulted in the increase in the compatibility amongst the Span 60 and the mustard oil molecules. The result supports the prediction of higher stability of the formulations made from the enthalpy values.

2-2. FTIR Studies

The interactions within the oleogel components were studied using FTIR analysis (Fig. S3). The absorption peak at 1,750 cm^{-1}

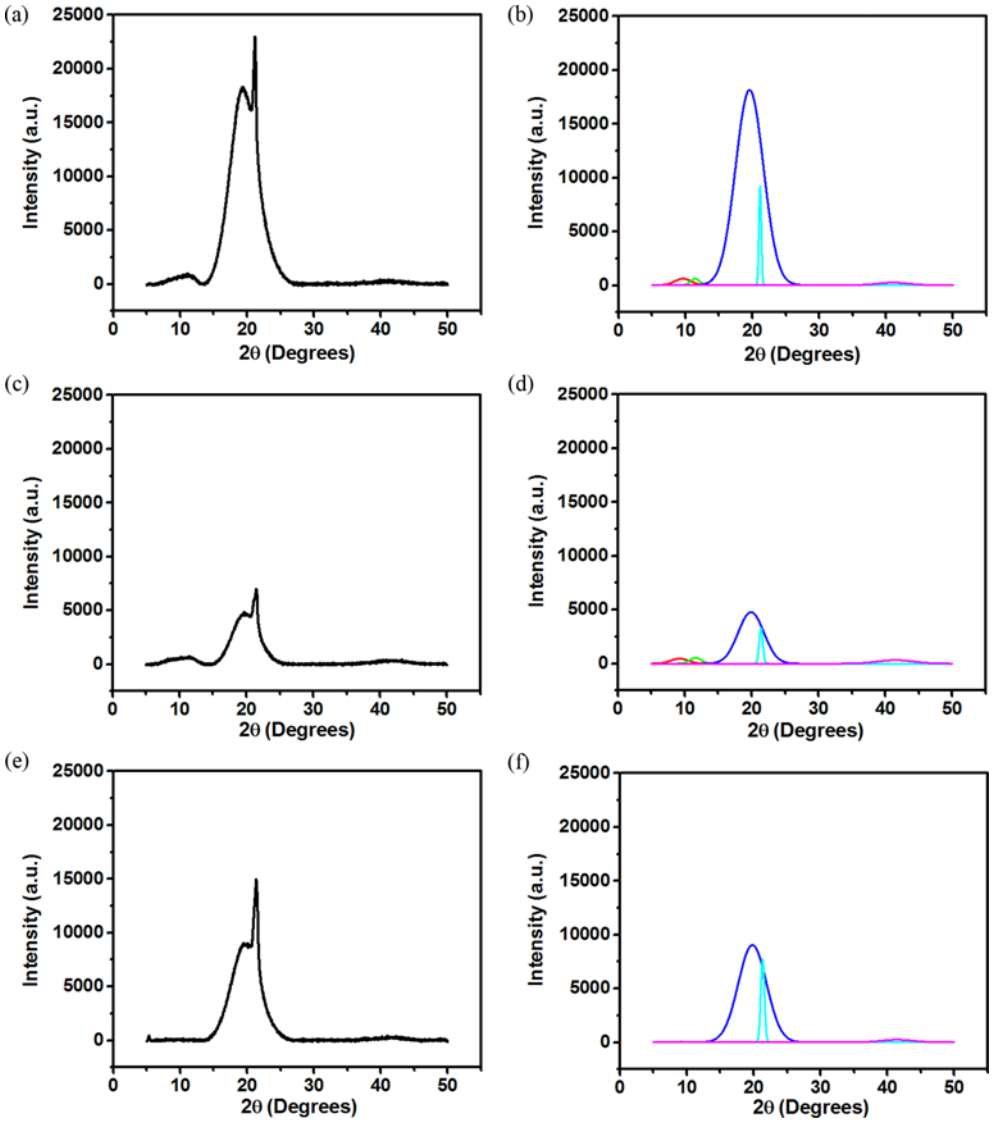

Fig. 3. XRD profiles of (a) F1; (b) deconvoluted peaks of F1; (c) F2; (d) deconvoluted peaks of F2; (e) F3; and (f) deconvoluted peaks of F3.

was due to CO stretching vibrations of the carboxylic group present in Span 60. The peak at 3,500 cm^{-1} was due to the presence of free hydroxyl groups in Span 60 [25]. The peak intensity of this peak was decreased in the oleogels with the increase in the Span 60 concentration. This suggested that the hydroxyl groups of Span 60 were involved in the formation of the gelator network [12,26].

2-3. XRD Studies

The XRD profiles of the oleogels are shown in Fig. 3. The underlying peaks of the profiles were determined using the peak-fitting tool of Origin Pro 2015 software [27]. The fitting was done using Gaussian function. From the analysis, there were five underlying peaks. The position of the peaks is tabulated in Table 2. The peak characteristics suggested an increase in the Span 60 concentration resulted in the major change in the intensity of P3 and P4 peaks. Hence for further analyses, P3 and P4 peaks were chosen. The full width at half maxima (FWHM) of P3 was higher than P4. This indicated that the crystallites resulting in the occurrence of P3 were comparatively amorphous as compared to P4. Hence, a ratio of peak intensity of P4 and P3 was calculated. The results suggested an increase in the relative crystallinity of the oleogels with the increase in the Span 60 concentration. The average d-spacing was nearly equal in all the three formulations, F1 (4.36 Å), F2 (4.30 Å) and F3 (4.32 Å), but a marked decrease in the average crystallite size of Span 60, F1 (11.03 nm), F2 (7.55 nm) and F3 (7.42 nm), was observed (Fig. S4) with the increase in the Span 60 concentration. The decrease in the crystallite size was much higher when the Span 60 concentration was increased from 17% (F1) to 20% (F2). A subsequent increase in the Span 60 concentration from 20% (F2) to 22% (F3) resulted in the gradual decrease in the crystallite size. This indicated that an increase in the Span 60 concentration did not favor crystal growth. The average lattice strain of F1, F2 and F3 was 0.066, 0.063 and 0.069, respectively (Fig. S4). It has been reported that a change in the lattice strain might affect the physical properties of the samples [28].

2-4. Mechanical Properties

The gel strength profiles showed an increase in the strength of

Table 2. XRD parameters

Formulations	Peaks	Peak position (2θ)	FWHM (2θ)	Peak Height (Intensity, a.u.)	Peak height ratio (P4/P3)	d-Spacing (Å)	Crystallite size (nm)	Lattice strain
F1	P1	9.63038	2.81246	584.27333	--	--	--	--
	P2	11.47305	1.55704	587.28246	--	--	--	--
	P3	19.58416	4.90649	18117.14824	--	4.53	1.72	0.124
	P4	21.17154	0.41528	9178.02227	--	4.19	20.33	0.0097
	P5	41.05217	5.04923	230.35778	--	--	--	--
					0.507			
F2	P1	9.23155	3.09603	477.33777	--	--	--	--
	P2	11.61153	2.06007	539.34287	--	--	--	--
	P3	19.90852	4.50618	4782.66881	--	4.4562	1.87	0.112
	P4	21.40178	0.63882	3287.33246	--	4.1485	13.22	0.0148
	P5	41.5334	6.44088	329.53169	--	--	--	--
					0.687			
F3	P1	9.19472	0.1094	83.30582	--	--	--	--
	P2	11.68681	0.03646	75.20943	--	--	--	--
	P3	19.81711	4.97014	9022.99988	--	4.4765	1.69	0.1241
	P4	21.3444	0.64268	7683.88736	--	4.1595	13.14	0.0149
	P5	41.45394	5.30554	238.57418	--	--	--	--
					0.851			

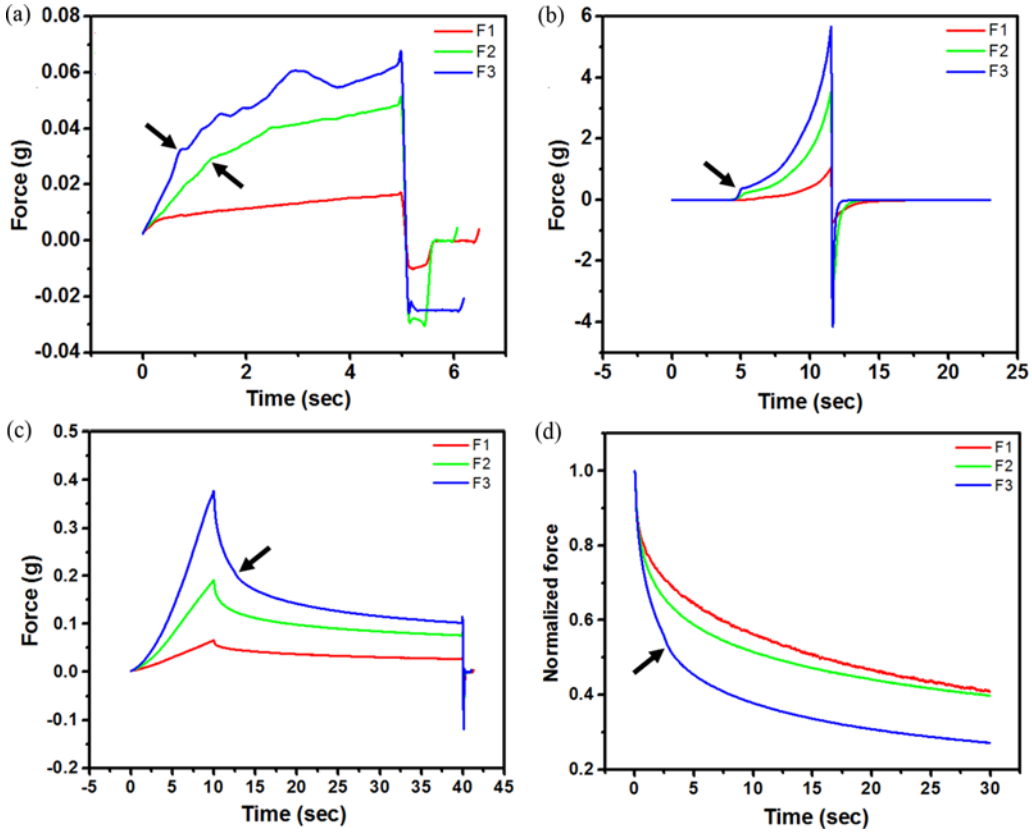

Fig. 4. (a) Gel strength profiles; (b) spreadability profiles; (c) stress relaxation profiles; and (d) normalized stress relaxation profiles.

the oleogels when the concentration of Span 60 was increased (Fig. 4(a)). An increase in the strength of the oleogels was associated with the increase in the brittleness of the oleogels, marked by inflections in the gel strength profile (shown by arrows). Similar to the gel strength studies, the spreadability studies also indicated that the firmness (marked by positive peak force) of the oleogels was

increased with the increase in the Span 60 concentration (Fig. 4(b)). The inverse of the area under the positive profile is a marker of the spreadability. It was observed from the profiles that there was an increase in the area under the positive peak at higher Span 60 concentrations. This indicated that the spreadability of the oleogels which contained higher proportion of Span 60 was lower. Additionally, the breakage of the network structure was observed in F2 and F3. This was marked by a sudden increase in the force profile (marked by arrow) near the toe of the positive profile.

The results of the stress relaxation studies (Fig. 4(c)-(d)) are tabulated in Table 3. The maximum force achieved during the compression stage is regarded as F_0. F_0 is an indicator of the firmness of the samples. Like the spreadability study, the stress relaxation study also suggested that the firmness of the oleogels was increased with the rise in the Span 60 concentration. The firmness (F_0) of the oleogels is in the order of F3>F2>F1. When the probe was held at the same position after reaching a distance of 10 mm, there was an exponential decrease of the force values to a residual force (F_r) [29]. The decay in the force values is due to the combined effect of molecular rearrangement of the oleogel components (specially the gelator molecules), disruption of the network structure and breaking of the gelator fiber structure. The residual force remaining after the completion of the test is a marker of the residual elastic component remaining within the samples. The decay profiles of the force were dependent on the composition of the oleogels. The decay profile of F3 showed a discontinuity during the relaxation process. This suggested breakage of the network structure when a constant stress was applied. The breakage of the network structure may be explained by the increased brittleness of the network structure when the concentration of the gelator was increased. The percent stress relaxation (%SR) was calculated using Eq. (1). The %SR provides information about the ability of the sample to absorb the energy associated with the induced strain. A higher %SR is observed in the materials having higher degree of fluidity or by a polymeric structure whose network undergo easy disruption. The %SR was higher in the oleogels which contained higher proportions of Span 60 (Table 3). F3 showed highest % SR as compared to F2 and F1. The %SR of F1 and F2 were closer to each other. But when the concentration of Span 60 was increased to 22% (F3) from 20% (F2), there was a drastic increase in the %SR. This can be explained by the breakage of the Span 60 network, as was observed from the relaxation profile of F3.

Table 3. Stress relaxation parameters

Analysis model	Parameters	Formulations		
		F1	F2	F3
--	F_0 (g)	0.066	0.191	0.377
	F_r (g)	0.027	0.076	0.102
	%SR	59.200	60.237	72.833
Weichert model	P_0	0.329	0.345	0.220
	P_1	0.125	0.189	0.365
	τ_1 (sec)	2.079	2.027	1.826
	P_2	0.393	0.299	0.2762
	τ_2 (sec)	18.916	17.434	17.417
	P_3	0.166	0.179	0.155
	τ_3 (sec)	0.182	0.227	0.187
	R^2	0.999	0.999	0.999

The stress relaxation profiles provide information about the viscoelastic nature of the samples. The information may be extracted using suitable models (e.g., Maxwell model, Kohlrausch model and Weichert model). In this study, the Weichert model of viscoelasticity was employed to have an understanding on the viscoelastic property of the oleogels. This is because the Weichert model is one of the most complex models and has been reported to predict the relaxation process with high accuracy. The relaxation profiles were initially normalized (Fig. 4(d)). The normalized profiles were fitted with Weichert model (Eq. (2)) of viscoelasticity (Table 3) [30]. P_0 is a marker of inherent mechanical stability of the oleogels. In other words, P_0 is a marker of the inherent elastic component which is retained after the relaxation process is complete. P_0 of F2 was highest amongst all the oleogels, which suggested that the inherent mechanical stability of F2 was highest followed by F1 and F3, respectively. This suggested that the molecular interactions amongst the gelator molecules achieved a critical higher limit in F2 as the gelator proportion was increased F1 to F2. Thereafter, a further increase in the gelator proportion in F3 made the gelator network structure brittle, which resulted in the breaking of the structure under strain. The higher mechanical stability of F2 may further be explained by the lowest lattice strain of the crystallites, which allowed the formation of a compact gelator network structure in F2. Instantaneous (τ_1), intermediate (τ_2) and delayed (τ_3) relaxation times were calculated. The τ_1 and τ_2 values of the oleogels were in the order of F1>F2>F3. On the other hand, τ_3 was in the order of F2>F3>F1. An increase in Span 60 concentration resulted in the decrease in the instantaneous and the intermediate relaxation times. This suggested a quick reorientation of the gelator molecules when Span 60 concentration was increased. The delayed relaxation time was much higher in F2 as compared to F1 and F3, which showed similar delayed relaxation time. Delayed relaxation time is a marker of gelator network physical stability when a stress is applied. A longer relaxation time suggests that the gelator network is able to maintain its structural integrity under stress condition for prolonged duration. This observation can explain the better inherent stability of F2 as was predicted from the P_0 values.

$$\%\ \text{relaxation} = \left(\frac{F_0 - F_r}{F_0}\right) * 100 \tag{1}$$

where, F_0 is the maximum force developed at each cycle; F_r is the force after time t at each cycle.

$$P_{(t)} = P_{(0)} + P_{(1)} \cdot e^{-t/\tau_1} + P_{(2)} \cdot e^{-t/\tau_2} + P_{(3)} \cdot e^{-t/\tau_3} \tag{2}$$

where, $P_{(0)}$, $P_{(1)}$, $P_{(2)}$ and $P_{(3)}$ are the spring constants; and τ_1, τ_2 and τ_3 are time constants of the dashpots.

2-5. *In vitro* Drug Release Studies

Fig. 5(a) shows the release profile of the drug (ciprofloxacin) from the oleogels. The release of the drug from F2 was highest as compared to F1 and F3, respectively, at the end of the experiment. The release profile was fitted with Korsmeyer-Peppas model (Eq. (3), Table 4) [31,32]. The Korsmeyer-Peppas model provides information on the diffusion of the drugs within the gel matrices. The model not only provides information on the diffusion coefficient

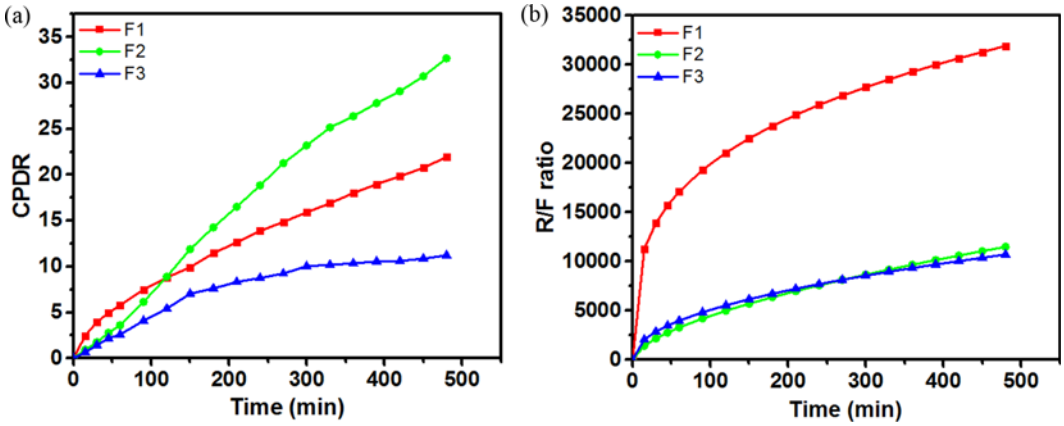

Fig. 5. Drug release properties. (a) Cumulative drug release (CPDR) profiles; and (b) R/F ratio profiles.

Table 4. Drug release parameters

Analysis model	Parameters	Formulations		
		F1	F2	F3
Korsmeyer-Peppas model	K	0.501	0.028	0.057
	n	0.599	1.201	0.949
	R^2	0.999	0.999	0.997
Peppas-Sahlin model	k_1	0.0001	0.0001	0.0001
	k_2	0.501	0.028	0.057
	m	0.299	0.600	0.474
	R^2	0.999	0.999	0.997

of the drug (also regarded as rate of drug diffusion), but also the nature of the diffusion (Fickian, Case-II or super Case-II). The prediction of the Korsmeyer-Peppas model parameters suggested that the rate of the drug diffusion (K) was highest in F1, followed by F3 and F2, respectively. The rates of the drug diffusion in F2 and F3 were nearly equal. Korsmeyer- Peppas model is used to model the release kinetics of the drug at initial stages [31]. A careful examination of the release profile during the first hour of the experimentation suggested that the release was fastest from F1 followed by F2 and F3, respectively, whose release was nearly equal. The diffusion exponent (n) of F1 and F3 suggested case-II diffusional transport, whereas the diffusion exponent of F2 suggested super case-II diffusional transport (Table 4). Case-II and super case-II diffusional transport usually happens due to the combination of Fickian diffusion and diffusion associated with the polymer chain relaxation. Hence, the release kinetics data were fitted with Peppas-Sahlin model (Eq. (4)). The parameters of the Peppas-Sahlin model (Table 4) were used for calculating R/F ratio (Diffusion due to relaxation: Fickian diffusion) profiles using Eq. (5) [33]. The R/F ratio profiles (Fig. 5(b)) suggested that the diffusion of the drugs due to polymer relaxation was more predominant in F1 as compared to F2 and F3, which showed nearly similar R/F ratio profiles. Since the R/F values were >1 in all the cases, it can be expected that the relaxation process of the gelator network was playing an important role in the drug release process. From the results, it can be concluded that an increase in the gelator concentration results in the decrease in the network flexibility and hence the polymer relaxation process.

$$CPDR = K \cdot t^n \quad (3)$$

where, CPDR=Cumulative percent drug release, K=Rate of drug diffusion, n=Diffusion exponent.

$$CPDR = k_1 \cdot t^m + k_2 \cdot t^{2m} \quad (4)$$

where, CPDR=Cumulative percent drug release, k_1=Rate of drug diffusion due to Fickian diffusion, k_2=Rate of drug diffusion due to polymer relaxation, and m=Composite diffusion exponent.

$$D = \frac{R}{F} = \frac{k_2 \cdot t^m}{k_1} \quad (5)$$

where, D=Ratio of diffusion factor due to relaxation process (R) and Fickian diffusion (F).

CONCLUSION

Span 60 based oleogels were developed by varying the proportions of Span 60. An alteration in the microstructure, molecular interaction, thermal properties and mechanical properties were investigated in-depth. The microscopic studies showed an increase in the density of the gelator network as the concentration of Span 60 was increased. The thermal analysis of the oleogels suggested that the crystallization of Span 60 during the process of gelation was a two-stage process. The two-stage crystallization process was confirmed from crystallization kinetics and DSC thermogram analysis. From the XRD studies, it was observed that there were two major peaks which correspond to the presence of Span 60 crystals of two sizes. At lower proportions of Span 60 two minor peaks were present, which vanished completely when the concentration of Span 60 was increased to 22% in F3. This is only possible when crystallization has occurred in a two-stage process. An in-depth analysis of the thermograms suggested an increase in the thermal compatibility among the components of the oleogels. The increase in the gelator network density resulted in the increase in the interconnecting points, which, in turn, increased the mechanical stability of the oleogels. Unfortunately, the increase in the mechanical property was also associated with the increase in the brittleness of the oleogels. An increase in the brittleness is usually associated with the breakage of the gelator network as stress is applied on the

formulations. In our study, during stress relaxation the relaxation time (instantaneous, intermediate and delayed) of F3 (containing 22% of Span 60) was least. Interestingly, the relaxation times of F1 and F2 were similar. This suggested that even though the brittleness of F2 was higher as compared to F1, the tendency to undergo disruption of the gelator network was not significantly different. The alteration in the mechanical properties may be explained by the alteration in the lattice strain of the gelator crystals present in the gelator network. It was found that the lattice strain was least in F2 followed by F1 and F3, respectively. A careful evaluation of the Weichert model parameters showed that the delayed relaxation time was highest in F2. Delayed relaxation time is a marker of network breakage at longer durations. This suggested that the inherent stability of the oleogels might be higher in F2. P_3 of F2 was highest amongst the three formulations. P_3 is a marker of inherent stability of the formulations at longer durations. The analysis of the XRD and Weichert model parameters suggested that the formation of crystals having lower lattice strain might result in the increase in the inherent mechanical stability of the oleogels. An in-depth analysis of the drug release profile suggested that the increase in the Span 60 proportion in the oleogels promoted Fickian diffusion of the drug. However, the diffusion of the drug due to the relaxation of the gelator network was significantly lowered when the Span 60 concentration was increased. Essentially, the crystallization of the gelator during the gelation process alters the crystallite sizes, which, in turn, not only alters the mechanical properties of the oleogels but also the release mechanics of the drugs.

ACKNOWLEDGEMENT

The authors acknowledge the National Institute of Technology (NIT), Rourkela, India for providing the logistic and instrumental facilities. The funds leveraged from the project (BT/PR14282/PID/06/598/2010) sanctioned by the Department of Biotechnology, Govt. of India are hereby acknowledged.

SUPPORTING INFORMATION

Additional information as noted in the text. This information is available via the Internet at http://www.springer.com/chemistry/journal/11814.

REFERENCES

1. P. F. Duan, Y. G. Li, J. Jiang, T. Y. Wang and M. H. Liu, *Sci. China Chem.*, **54**, 1051 (2011).
2. S. Raut, S. S. Bhadoriya, V. Uplanchiwar, V. Mishra, A. Gahane and S. K. Jain, *Acta Pharmaceutica Sinica B* (2012).
3. H. Sawalha, P. Venema, A. Bot, E. Flöter and E. van der Linden, *Food Biophysics*, 1 (2011).
4. N. Dew, K. Edsman and E. Björk, *J. Pharm. Pharmacol.*, **63**, 1265 (2011).
5. I. Effendy and H. I. Maibach, *Contact Dermatitis*, **33**, 217 (1995).
6. A. Lips, K. Ananthapadmanabhan, M. Vetamuthu, X. Hua, L. Lang and C. Vincent, *Surfactants in Personal Care Products and Decorative Cosmetics*, 177 (2010).
7. M. Carafa, C. Marianecci, F. Rinaldi, E. Santucci, S. Tampucci and D. Monti, *J. Liposome Res.*, **19**, 332 (2009).
8. L. Fengyan, Z. Wenli, Z. Tianbo, D. Danghui and Y. Fang, *Factors influencing droplet size of silicone oil emulsion with high solid content* (2011).
9. V. B. Junyaprasert, P. Singhsa, J. Suksiriworapong and D. Chantasart, *Int. J. Pharm.*, **423**, 303 (2012).
10. R. Villalobos-Carvajal, P. Hernández-Muñoz, A. Albors and A. Chiralt, *Food Hydrocolloids*, **23**, 526 (2009).
11. L. Wang, J. Dong, J. Chen, J. Eastoe and X. Li, *J. Colloid Interface Sci.*, **330**, 443 (2009).
12. M. A. Rogers, *Food Res. Int.*, **42**, 747 (2009).
13. A. Jain, A. Jain, A. Gulbake, S. Shilpi, P. Hurkat and S. K. Jain, Peptide and protein delivery using new drug delivery systems, *Critical Reviews™ in Therapeutic Drug Carrier Systems* **30** (2013).
14. E. S. Kimball, N. K. Wallace, C. R. Schneider, M. R. D'Andrea and P. J. Hornby, *Frontiers in Gastrointestinal Pharmacology*, **1** (2010).
15. M. Turgis, J. Han, S. Caillet and M. Lacroix, *Food Control*, **20**, 1073 (2009).
16. M. Yu and M. Vajdy, *Vaccine*, **29**, 2429 (2011).
17. I. Shaikh, K. Jadhav and V. Kadam, Lecithin organogels in enhancing, *Percutaneous Penetration Enhancers Chemical Methods in Penetration Enhancement: Drug Manipulation Strategies and Vehicle Effects*, 299 (2015).
18. J. A. Paice, *Pain Management Nursing*, **6**, 145 (2005).
19. W. A. Ritschel, W. Ye, L. Buhse and J. C. Reepmeyer, *Int. J. Pharm.*, **362**, 67 (2008).
20. N. Fujita and S. Shinkai, *Molecular gels*, Weiss, R. and Terech, P., Eds., Springer Netherlands, 553 (2006).
21. M. M. Talukdar, I. Vinckier, P. Moldenaers and R. Kinget, *J. Pharm. Sci.*, **85**, 537 (1996).
22. S. Murdan, G. Gregoriadis and A. T. Florence, *J. Pharm. Sci.*, **88**, 608 (1999).
23. D. C. Zulim Botega, A. G. Marangoni, A. K. Smith and H. D. Goff, *J. Food Sci.*, **78**, C1334 (2013).
24. M. A. Bootello, R. W. Hartel, R. Garcés, E. Martínez-Force and J. J. Salas, *Food Chem.*, **134**, 1409 (2012).
25. X. Xu, M. Ayyagari, M. Tata, V. T. John and G. L. McPherson, *J. Phys. Chem.*, **97**, 11350 (1993).
26. A. Vintiloiu and J.-C. Leroux, *J. Controlled Release*, **125**, 179 (2008).
27. X. D. Hou, T. J. Smith, N. Li and M. H. Zong, *Biotechnology and Bioengineering*, **109**, 2484 (2012).
28. N. Farhadyar, M. Sadjadi, F. Farhadyar and A. Farhadyar, *J. Nano Res.*, Trans Tech Publish, 51 (2013).
29. B. Roopa and S. Bhattacharya, *J. Food Eng.*, **131**, 38 (2014).
30. S. Meghezi, F. Couet, P. Chevallier and D. Mantovani, *Int. J. Biomaterials*, **2012** (2012).
31. H. Jian, L. Zhu, W. Zhang, D. Sun and J. Jiang, *Carbohydrate Polymers*, **87**, 2176 (2012).
32. N. A. Peppas and B. Narasimhan, *J. Controlled Release*, **190**, 75 (2014).
33. I. Popescu, I. M. Pelin, M. Butnaru, G. Fundueanu and D. M. Suflet, *Carbohydr. Polym.*, **94**, 889 (2013).

Supporting Information

Effect of sorbitan monostearate concentration on the thermal, mechanical and drug release properties of oleogels

Sai Sateesh Sagiri*, Uvanesh Kasiviswanathan*, Gauri Shankar Shaw*, Meenakshi Singh*, Arfat Anis,†, and Kunal Pal*,†**

*Department of Biotechnology and Medical Engineering, National Institute of Technology, Rourkela-769008, Orissa, India
**SABIC Polymer Research Center, Department of Chemical Engineering, King Saud University, Riyadh-11421, Saudi Arabia
(*Received 11 September 2015 • accepted 23 December 2015*)

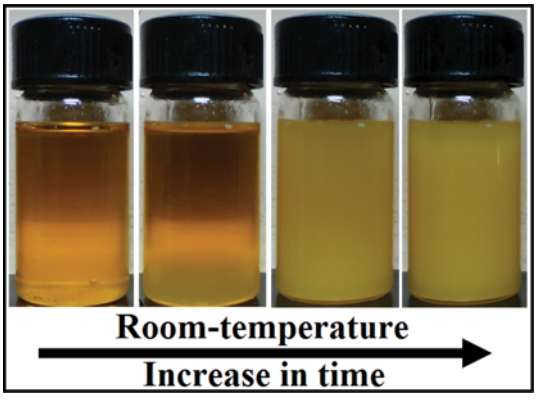

Fig. S1. Stages during the gelation process.

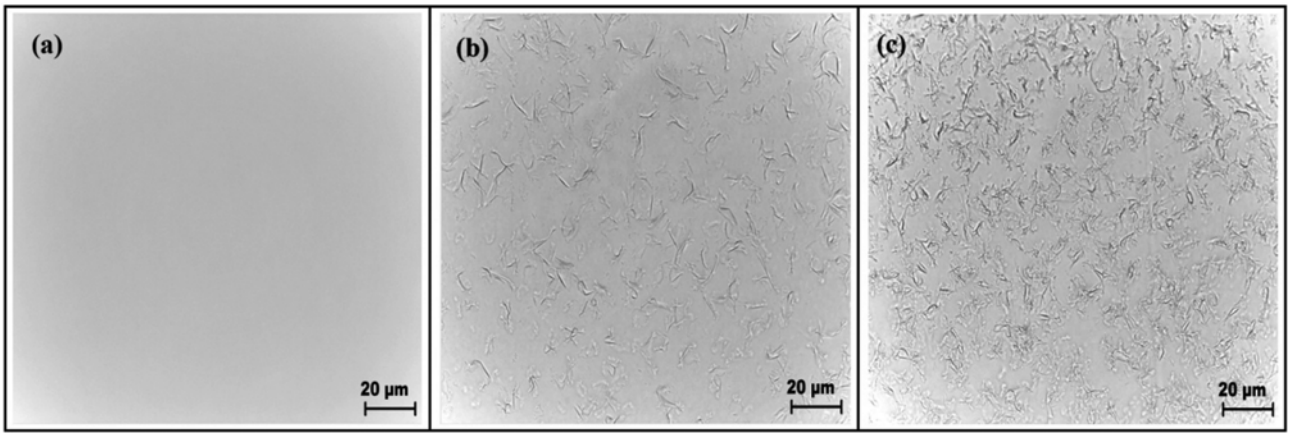

Fig. S2. Alteration in the microstructure during cooling of the hot solution of Span 60.

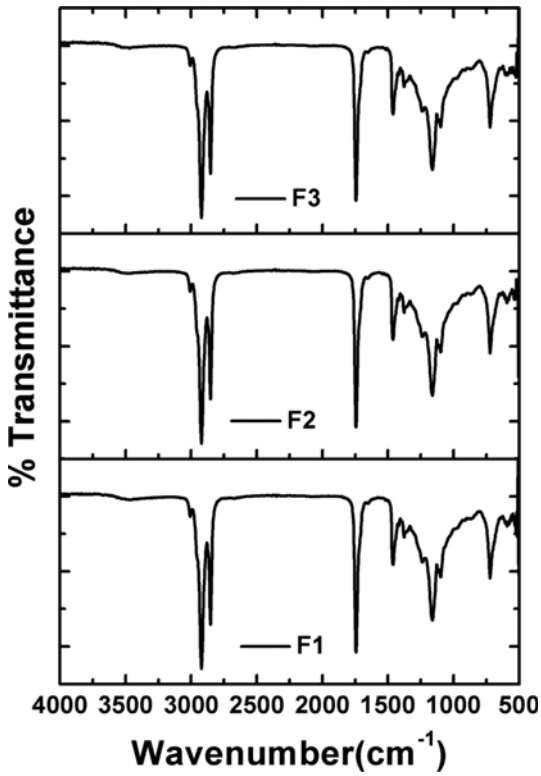

Fig. S3. FTIR spectra of: (a) F1; (b) F2; and (c) F3.

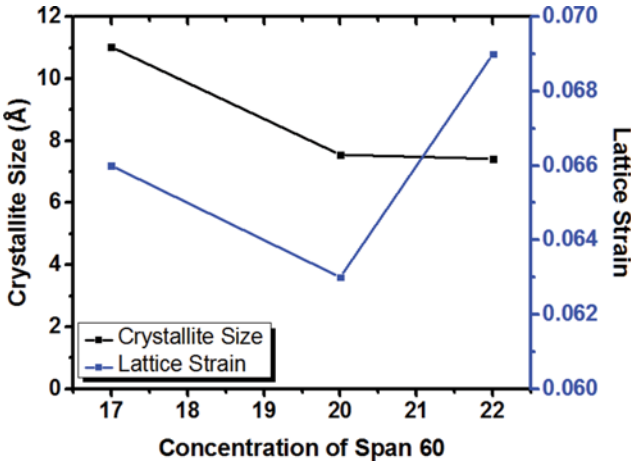

Fig. S4. Variation in the crystallite size and crystal strain as a function of Span 60 concentration.

Table S1. Thermal parameters

Formulations	Melting parameters			Crystallization parameters		
	T_{m1}	T_{m2}	ΔH_m	T_{c1}	T_{c2}	ΔH_c
F1	51.7	56.4	12.06	45.2	39.6	1.484
F2	50.7	55.9	13.35	45.8	39.9	1.632
F3	51.8	56.7	14.15	45.8	40.2	2.158